Published in final edited form as:
Oncogene. 2013 March 7; 32(10): 1223–1232. doi:10.1038/onc.2012.145.

A20/TNFAIP3 inhibits NF-κB activation induced by the Kaposi's sarcoma-associated herpesvirus vFLIP oncoprotein

S Sakakibara[1,3], **G Espigol-Frigole**[1,3], **P Gasperini**[1], **TS Uldrick**[2], **R Yarchoan**[2], and **G Tosato**[1]

[1]Laboratory of Cellular Oncology, Center for Cancer Research, National Cancer Institute, National Institutes of Health, Bethesda, MD, USA

[2]HIV and AIDS Malignancy Branch, Center for Cancer Research, National Cancer Institute, National Institutes of Health, Bethesda, MD, USA

Abstract

Kaposi's sarcoma-associated herpesvirus (KSHV) K13/vFLIP (viral Flice-inhibitory protein) induces transcription of numerous genes through NF-κB activation, including pro-inflammatory cytokines, which contribute to the pathogenesis of Kaposi's sarcoma (KS). In this study, we report that KSHV vFLIP induces the expression of the NF-κB regulatory proteins A20, ABIN-1 and ABIN-3 (A20-binding NF-κB inhibitors) in primary human endothelial cells, and that KS spindle cells express A20 in KS tissue. In reporter assays, A20 strongly impaired vFLIP-induced NF-κB activation in 293T cells, but ABIN-1 and ABIN-3 did not. Mutational analysis established that the C-terminal domain (residues 427–790) is critical for A20 modulation of NF-κB, but the ubiquitin-editing OTU (ovarian tumor) domain is not. In functional assays, A20 inhibited vFLIP-induced expression of the chemokine IP-10, reduced vFLIP-induced cell proliferation and increased IKK1 protein levels. Thus, we demonstrate that A20 negatively regulates NF-κB activation directly induced by KSHV vFLIP. By attenuating excessive and prolonged vFLIP-induced NF-κB activation that could be harmful to KSHV-infected cells, A20 likely has an important role in the pathogenesis of KSHV-associated diseases, in which vFLIP is expressed.

Keywords

KSHV; NF-κB; vFLIP/K13; endothelial cells; Kaposi's sarcoma; AIDS

INTRODUCTION

Kaposi's sarcoma-associated herpesvirus (KSHV) is the etiological agent of Kaposi's sarcoma (KS), primary effusion lymphoma (PEL), a subset of multicentric Castleman's disease and an (interleukin) IL-6-related inflammatory syndrome associated with AIDS.[1,2] In these malignancies, KSHV establishes a mostly latent infection where transcription of viral genes is limited.[3] *ORF K13,* one of the few KSHV genes expressed during latency, is believed to have important roles in viral persistence and disease pathogenesis.[4–8] For example, the growth and survival of PEL cells in culture is dependent upon continued

Correspondence: Dr G Espigol-Frigole, Laboratory of Cellular Oncology, CCR, NCI, NIH; Building 37, Room 4134, Bethesda, MD 20892, USA. GESPIGOL@clinic.ub.es.

[3]These authors contributed equally to this work

CONFLICT OF INTEREST

The authors declare no conflict of interest.

expression of the KSHV *K13 gene* product, named vFLIP (for viral Flice-inhibitory protein)/K13 protein.[9]

The vFLIP protein activates the canonical NF-κB pathway through direct binding to NEMO (NF-κB essential modulator, also known as IKKγ), which functions as a regulatory subunit of the IKK (IκB kinase) complex.[10,11] The IKK complex, composed of two catalytic subunits, IKKα and IKKβ, and the scaffolding subunit IKKγ/NEMO, phosphorylates IκBα (inhibitor of NF-κB) at specific serine residues.[12–16] This leads to the ubiquitin/proteasome-dependent degradation of IκBα, and to release of NF-κB components such as RelA/p65 and p50, which subsequently translocate to the nucleus where they function as DNA-binding transcription factors.[17]

Expression of vFLIP in primary endothelial cells activates NF-κB resulting in increased transcription of inflammatory cytokines (IL-1, IL-6, granulocyte-macrophage colony-stimulating factor and others), chemokines (RANTES, IP-10 and others), interferon-induced anti-viral genes (Mx1, ISG15 and others) and other genes.[18–22] In previous studies, we found that vFLIP promotes the endothelial cell expression of certain NF-κB signaling modulators, including A20 (also known as tumor necrosis alpha-induced protein 3, TNFAIP3), ABIN-1 (A20 binding inhibitor of NF-κB 1), ABIN-3, IκBα, cIAP2 and TRAF1 (TNFR-associated factor 1).[21] Recently, vFLIP was reported to promote A20 expression in PEL cells.[23]

A20 is a zinc finger protein identified in endothelial cells stimulated with TNFα,[24] which inhibits TNFα-induced cell death by blocking NF-κB activation.[25,26] Subsequent experiments showed that NF-κB activates A20 expression with the contribution of the transcriptional apparatus, certain transcription factors and co-activators.[27,28] Biochemical and genetic studies indicated that A20 downregulates NF-κB signaling through the combined activity of its two distinct ubiquitin-editing domains at the N- and C-terminus.[29,30] Other studies showed that A20 regulates LPS-TLR4-induced signaling, and that the carboxy-terminal domain of A20 is sufficient to inhibit LPS-TLR4-induced NF-κB activation.[31] A20 has several binding partners, including the E3 ubiquitin ligases TRAF1, TRAF2, TRAF6, Itch and RNF11, and other proteins, including TAXBP1 (Tax-binding protein) and A20-binding NF-κB inhibitors (ABINs), suggesting the potential for complex functional interactions.[32–35] The ABIN proteins (ABIN-1, -2 and -3) were originally identified as NF-κB inhibitors, which bind A20 through the ABIN homology domain-1.[28,33,36,37] Expression of ABIN-1 and ABIN-3 is regulated by NF-κB.[28,37–39]

In the present study, we examined the relationship between KSHV vFLIP and A20, ABIN-1 and ABIN-3, and analyzed the potential roles of these NF-κB regulators in KSHV infection of endothelial cells. We show that A20 functions as a negative regulator of KSHV vFLIP-induced NF-κB activation, modulating chemokine secretion and cell growth. Furthermore, we find that A20 is expressed in KSHV-infected cells within KS tissue. These results support an important modulatory role for A20 in the context of KS pathogenesis.

RESULTS

Transduction of KSHV vFLIP in endothelial cells activates the NF-κB pathway and stimulates expression of A20, ABIN-1 and ABIN-3 We transduced the KSHV *vFLIP* gene in primary human umbilical vein endothelial cells (HUVEC) using the Ires-Gfp retroviral vector (LZRSpBMN-ORF13-Ires-GFP) described previously.[21] Expression of vFLIP was reflected by GFP fluorescence detected by microscopy 24 h after infection of HUVEC (Figure 1a). We examined early changes in expression of selected cellular proteins, with a focus on components of the canonical NF-κB pathway (Figure 1b), which is activated by

vFLIP.[7,10] Phosphorylation of the inhibitory protein IκBα, a critical step for release and nuclear translocation of NF-κB components, was first detected 24 h after transduction with vFLIP-retrovirus but not control retrovirus. Expression of some of the NF-κB target genes was induced early, as evidenced by increased protein levels of COX2 and RelB 24–48 h after vFLIP transduction. Expression of the NF-κB target gene p100/NF-κB2 was detected at low levels 48 h and 72 h after transduction with vFLIP but not control retrovirus. As we previously reported,[21] vFLIP induced STAT1 phosphorylation after 48 h, somewhat later than IκBα phosphorylation. vFLIP also induced ERK1/2 phosphorylation, which was sustained over 72 h. Consistent with activation of the NF-κB canonical pathway, vFLIP-transduced HUVEC displayed p65/RelA in the nucleus, whereas control cells displayed p65/RelA in the cytoplasm (Figure 1c).

Expression of the NF-κB target chemokine genes IP-10 and MCP2 was evaluated by measuring mRNA and protein levels in HUVEC transduced with vFLIP. IP-10 and MCP2 mRNAs were first detected 24–48 h after vFLIP transduction, peaked at 72–96 h, and decreased by 144 h (Figure 1d). Consistent with this pattern of mRNA kinetic expression, IP-10 and MCP2 proteins were first detected in the culture supernatant after 48–72 h, peaked at 72–96 h and decreased by 144 h (Figure 1e). Levels of phosphorylated IκBα protein (Figure 1b) also decreased by 144 h after vFLIP transduction (not shown). This suggested the occurrence of a negative feedback loop inhibiting NF-κB activation and expression of IP-10 and MCP2 in HUVEC.

On the basis of a microarray analysis, we previously reported that vFLIP enhances the expression of A20/TNFAIP3 (TNFα-induced protein 3) and ABIN-3 (A20-binding NF-κB inhibitor 3), and moderately enhances the expression of ABIN-1 in endothelial cells.[21] Expression of ABIN-2 was very low or undetectable in vFLIP-expressing endothelial cells (not shown). To confirm that vFLIP induces the expression of these genes, we used RT–PCR analysis and immunoblotting. When vFLIP or vector-only expression was detected in 76–96% of HUVEC (Figure 2a), the mRNAs of A20, ABIN-1 and ABIN-3 were markedly increased in vFLIP-expressing HUVEC compared with control (Figure 2b). The A20 protein was detected in vFLIP-transduced HUVEC at much higher levels than in vector-only expressing cells (Figure 2b). Similarly, vFLIP was reported to upregulate A20 expression in PEL cells.[23]

vFLIP is generally expressed in KS tissues.[8] We examined whether A20 is also expressed in KS tissues. Using immunofluorescence microscopy, we easily detected A20 protein in these tissues (representative example, Figure 2c). Double staining for KSHV-LANA indicated that a proportion of cells in which A20 is detected are infected with KSHV. These KSHV-infected cells resembled morphologically KS spindle cells.[8] At the margins of KS lesions where LANA-positive cells are rare, a few A20-positive CD31-positive endothelial cells were also identified (Figure 2c), likely reflecting normal capillary endothelium. Thus, A20 is expressed in KSHV-infected KS lesions.

A20 inhibits vFLIP-induced NF-κB activation and IP-10 secretion A20, ABIN-1 and ABIN-3 were reported to inhibit NF-κB activation induced by TNFα or LPS.[29,37–40] To test whether A20, ABIN-1 and ABIN-3 can also inhibit NF-κB activation induced by vFLIP, we used luciferase reporter assays. Expression of vFLIP in 293T cells activated NF-κB-driven luciferase activity by approximately 65-fold. The HA (hemagglutinin)-tagged A20 reduced this vFLIP-induced luciferase activity, reflective of NF-κB inhibition (Figure 3a). Expression of ABIN-1 (HA-tagged) in 293T cells partially reduced vFLIP-induced NF-κB activation, whereas expression of ABIN-3 (Myc-tagged) was not inhibitory (Figure 3a). However, A20, ABIN-1 and ABIN-3 all effectively inhibited TNFα-induced NF-κB activation in 293T cells (Figure 3b).

We examined whether A20 can inhibit vFLIP-induced IP-10 secretion in 293T cells. Previous studies documented that the IP-10 promoter region contains two kappa B sites that control interferon gamma and LPS-induced IP-10 transcription.[41] We and others have established that IP-10 is rapidly induced by vFLIP expression in endothelial cells.[20,21] By enzyme-linked immunosorbent assay (ELISA), we confirmed that vFLIP expression induces IP-10 (~130 pg/ml) release in the culture supernatant of 293T cells (Figure 3c). A vFLIP mutant (A57L)[21] that fails to bind NEMO and does not activate the canonical NF-κB pathway induced minimal release of IP-10 from 293T cells (Figure 3c), indicating that the vFLIP-NEMO axis is the predominant contributor to NF-κB activation here. In this system, we observed that A20 inhibited IP-10 production (Figure 3c) induced by vFLIP through NF-κB activation. Similarly, A20 inhibited vFLIP-induced IL-8 and MIP3α production in 293T cells.[23]

The C-terminal domain of A20 is required for inhibition of vFLIP-induced NF-κB activity

vFLIP binds to the IKK complex (composed of IKKα, IKKβ and IKKγ/NEMO subunits) through NEMO. Because A20 also binds to NEMO,[42] we examined whether A20 inhibits vFLIP-induced NF-κB activity by competing with vFLIP for binding to NEMO. Therefore, we co-transfected 293T cells with V5-tagged vFLIP and FLAG-tagged NEMO with or without HA-tagged A20 (Figure 4a). Immunoprecipitation of vFLIP with an anti-V5 antibody followed by immunoblotting showed the expected presence of vFLIP and NEMO in the immunoprecipitates. Importantly, the amount of vFLIP and NEMO proteins detected in the precipitates was similar with or without expression of A20. This indicated that A20 does not prevent or reduce vFLIP binding to NEMO. Similarly, other studies have shown that A20 does not physically disrupt the vFLIP-IKK complex.[23] In addition, we detected little or no A20 protein after immunoprecipitation of vFLIP in 293T cells that expressed A20 and vFLIP, suggesting that A20 does not directly bind to vFLIP. This conclusion contrasts with the results showing that A20 directly interacts with vFLIP in PEL cell lines.[23] Endogenous IKKα was also co-precipitated with vFLIP with little interference by A20. Although Hsp90 was reported to bind the vFLIP-NEMO complex,[11] we could not detect Hsp90 in the precipitate of V5 antibody.

Previous studies provided evidence that vFLIP binds to TRAF2 (TNF receptor-associated factor 2),[7,43] but the role of TRAF2 in vFLIP-induced activation of the NF-κB pathway is controversial.[19] We examined the effects of A20 on the binding of vFLIP to TRAF2 (Figure 4b). By immunoprecipitation, we find that vFLIP binds to TRAF2, but that A20 does not alter this binding. These results provide evidence that A20 does not inhibit vFLIP-induced NF-κB activation by competing with vFLIP for binding to NEMO, by competing for vFLIP binding to TRAF2 or by directly binding to vFLIP.

A20 is a ubiquitin-editing enzyme that inhibits NF-κB activity through opposing effects on ubiquitination: at the amino-terminus, A20 contains a conserved motif, called OTU domain, responsible for the de-ubiquitination of lysine 63-linked chains; at the carboxy-terminus, A20 contains a zinc-finger motif that displays ubiquitin ligase activity inducing polyubiquitination and proteosomal degradation of receptor interacting protein (RIP). A previously described mutation in the OTU motif (D100A/C103S; aspartic acid 100 replaced with alanine and cysteine103 replaced with serine) disrupted the ability of A20 to de-ubiquitinate NEMO/IKKγ resulting in the loss of A20 inhibition of NF-κB activity.[38,44] To examine the importance of the OTU domain in the regulation of vFLIP-induced NF-κB activity, we tested A20 mutants in reporter assays. The A20 D100A/C103S mutant that lacks de-ubiquitination activity inhibited vFLIP-induced NF-κB activity as strongly as wild-type A20 (Figure 4c). By contrast, a large deletion of the C-terminal ubiquitin ligase domain (aa 428–790) markedly reduced the inhibitory effect of A20 (Figure 4c). Thus, these results

indicate that the de-ubiquitination activity of A20 is not required for inhibition of vFLIP-induced NF-κB activity.

As the large deletion at the carboxy-terminus, which contains the zinc finger domains 1–7, reduced A20 inhibitory activity of vFLIP-driven NF-κB activation, we next tested the effect of point mutations within the zinc-finger domains. We selected a minimal mutation (C624A/C627A) at zinc finger motif 4 (ZNF4), which was previously reported to attenuate the ubiquitination activity of A20[29] and a previously untested mutation (C779A/C782A) in zinc finger motif 7 (ZNF7). As shown in Figure 4d, the A20 ZNF4 mutant was as effective as WT A20 and the ZNF7 mutant at reducing vFLIP-induced NF-κB activity. These results demonstrate that the carboxy-terminal residues 428–790 are critical for A20 inhibition of NF-κB activation induced by vFLIP, and suggest that this activity of A20 is independent of its de-ubiquitinating and ubiquitinating functions.

A20, but not ABIN-1, regulates cell growth in vFLIP-expressing cells

NF-κB regulates growth in various cell types, including KSHV-infected PEL cells.[7,10,43] As we demonstrated that A20 serves as a negative regulator of vFLIP-induced NF-κB activity in model systems, we tested the effects of A20 on the proliferation of cells that express vFLIP.

We used the endothelial-like cell line EA.hy926 (EAHY) transduced with a vFLIP lentivirus as we could not perform these experiments in primary endothelial cells due to extensive cell death following vFLIP transduction[21] combined with A20 silencing. We achieved high-level vFLIP expression in EAHY cells as assessed by quantitative PCR analysis (Figure 5a, top panel), which was associated with increased expression of endogenous A20 (Figure 5a, bottom panel). The silencing lentivirus vectors shA20-1 and shA20-2 reduced expression of A20 in vFLIP-expressing EAHY cells as assessed by quantitative PCR (Figure 5a, bottom panel) and immunoblotting (Figure 5b). Proliferation assays using ^{3}[H] thymidine incorporation showed that A20 silencing increases significantly ($P<0.05$) the proliferation of vFLIP-expressing EAHY cells in comparison with control EAHY cells (Figure 5c), but minimally affects the proliferation of EAHY cells that do not express vFLIP (not shown). These results show that the silencing of A20 promotes the proliferation of EAHY cells that express vFLIP. Consistent with these results, the forced expression of A20 in vFLIP-Rat1 fibroblasts reduced soft-agar colony formation.[23]

Taking advantage of EAHY cells stably expressing vFLIP, we further explored the mechanisms underlying A20 regulation of cell growth. As shown (Figure 5d), vFLIP expression in EAHY cells was associated with increased IKK1 protein levels in comparison with control cells (not expressing vFLIP), whereas levels of IKK2 and NEMO protein levels minimally differed. The silencing of A20 in these cells selectively reduced IKK1 protein levels but not the levels of IKK2 or NEMO (Figure 5d). These results indicated that A20 regulates IKK1 protein levels in these cells, and raised the possibility that IKK1 may contribute to A20 modulation of cell growth in this system. To test for this possibility, we examined the effects of IKK1 silencing on EAHY cell proliferation. By using a pool of silencing RNAs (siRNAs), we effectively and specifically reduced IKK1 expression in vFLIP-expressing EAHY cells (Figure 5e). In proliferation assays, the knockdown of IKK1 significantly ($P<0.05$) enhanced the proliferation of EAHY cells compared with the control (Figure 5f), albeit to a somewhat lower degree than the silencing of A20 (Figure 5c). Instead, the knockdown of IKK1 failed to enhance the proliferation of EAHY cells that do not express vFLIP (not shown). These results support a role for IKK1 as a contributor to A20 modulation of cell growth in vFLIP-expressing EAHY cells.

To examine the specificity of A20-induced growth modulation, we silenced expression of ABIN-1 in EAHY cells that express vFLIP. The silencing lentiviral vectors shABIN-1a and shABIN-1b reduced expression of ABIN-1 in vFLIP-expressing EAHY cells as assessed by quantitative PCR (Figure 5g) and immunoblotting (Figure 5h). In addition, ABIN-1 silencing minimally altered the proliferation of vFLIP-expressing EAHY cells (Figure 5i). Thus, we conclude that A20 is a specific negative regulator of cell proliferation in endothelial cells that express vFLIP.

DISCUSSION

We report that the KSHV latency gene vFLIP promotes the expression of A20, a previously identified zinc-finger protein that inhibits NF-κB activity,[31] and that A20 can inhibit NF-κB activation induced by KSHV vFLIP in endothelial cells. As a similar inhibitory effect of A20 was recently described also in PEL,[23] the current results provide evidence for a broader role of vFLIP-induced A20 activation in KSHV-associated diseases, including KS. Thus, KSHV vFLIP can exert seemingly opposing effects on the NF-κB pathway, as it can directly promote NF-κB activation by binding to NEMO, the regulatory subunit of the IKK complex, and can indirectly inhibit NF-κB activation by inducing expression of A20. KSHV vFLIP and vFLIP-induced A20 bind to NEMO/IKKγ. However, we find that A20 does not compete with vFLIP for binding to NEMO, providing evidence that KSHV can target the NF-κB pathway at different points. By directly activating the NF-κB pathway thereby inducing cell growth and cytokine production, and indirectly reducing NF-κB activity thereby modulating cell growth and cytokine production, KSHV vFLIP likely has important regulatory functions for the survival and spread of KSHV in humans.

Analysis of the crystal structure of vFLIP binding to the IKK complex, which consists of IKKα/β and NEMO/IKKγ, suggested that the conformational change induced by vFLIP binding to NEMO resembles the conformational change occurring in NEMO during physiological activation of the canonical NF-κB pathway by inflammatory responses.[12] In inflammation, TNFα engagement of TNFR1 induces the assembly of a proximal signaling complex that includes of RIP, which becomes polyubiquitinated at Lys63 and recruits NEMO.[45] Non-covalent binding of linear or K63-linked ubiquitin to NEMO would determine a conformational change believed to be essential for the recruitment and the IKKα/β kinases and subsequent NF-κB activation.[46–48] A20 can bind to NEMO at residues 95–218 (included in the CC1 and HLX2 regions), a similar binding site to that of the linear ubiquitin chain and vFLIP,[46] but we found no evidence of competition between vFLIP and A20 for binding to NEMO. Similarly, A20 failed to physically disrupt the vFLIP-IKK complex.[23]

When TNFR signaling is induced, A20 inhibits NF-κB activation by targeting TNFR-associated RIP through the combined effects of the two ubiquitin-editing enzymes: the N-terminal A20 domain (OTU domain) removes Lys63-linked ubiquitin chains from RIP preventing its binding to NEMO, and the C-terminal A20 domain, composed of seven zinc fingers, conjugates Lys48-linked ubiquitin chains to RIP promoting its proteosomal degradation.[29] When vFLIP is expressed, binding to RIP is unlikely the mechanism by which A20 inhibits NF-κB activation because RIP does not contribute to vFLIP activation of the NF-κB pathway.[49] Other studies indicated that A20 inhibits the Toll-like receptor pathway of NF-kB activation by antagonizing interactions of TRAF2, TRAF6 and cIAP1 with the ubiquitin-conjugating enzymes Ubc13 and UbcH5c.[40] We considered the possibility that TRAF2 might be a target for A20 when vFLIP-induces NF-κB activation, as we found that vFLIP strongly binds to TRAF2. However, A20 did not compete for vFLIP binding to TRAF2. In addition, based on mutational analysis we conclude that the OTU domain and the C-terminal zinc finger 4 motif are not required for A20 inhibition of vFLIP-

induced NF-κB activation. However, other studies concluded that the N-terminal (1–380) and C-terminal (373–790) domains contribute to A20 inhibition of vFLIP-induced NF-κB activation.[23]

Taking advantage of an endothelial-like cell line, EAHY, in which stable expression of vFLIP was achieved to mimic more closely persistent expression of this gene as seen in natural KSHV infection, we noticed that IKK1 protein levels were selectively increased as a consequence of A20 expression. The silencing of IKK1 in these vFLIP-expressing EAHY cells was associated with increased cell proliferation similar to the effect of A20 silencing in these cells, pointing to a potential role for IKK1 as a mediator of A20 inhibition of NF-κB activation induced by vFLIP. Additional studies will be required to elucidate the mechanisms by which A20 increases IKK1 levels and the mechanisms by which IKK1 inhibits vFLIP-induced NF-κB activation. It is notable that IKK1 has been reported to be a negative regulator of canonical NF-κB activity in other contexts.[50–52] For example, macrophages from IKK1-null mice show greater production of pro-inflammatory cytokines as a result of canonical NF-κB activation.[51] In addition, IKK1 has been shown to inhibit NF-κB and inflammatory signaling by phosphorylating PIAS1, an inhibitor of STAT1 activation.[52] Furthermore, IKK1 has been shown to phosphorylate TAX1BP1 thereby negatively regulating NF-κB canonical signaling.[50]

We find that KSHV vFLIP promotes the expression of ABIN-1 (A20-binding inhibitor of NF-κB-1) and ABIN-3. The three ABIN proteins (ABIN-1, -2, and -3) were originally identified as NF-κB inhibitors that bind A20 through the ABIN homology domain 1.[28,33,36] Here, we find that ABIN-1 only modestly inhibited vFLIP-induced NF-κB activation and ABIN-3 did not inhibit. In addition, ABIN-1 silencing did not change the proliferation of vFLIP-expressing endothelial cells, and thus the function of ABIN-1 and ABIN-3 in KSHV infection remains to be defined.

What is the role of A20 in the context of endothelial cell infection with KSHV? Previous studies have illustrated that A20 is a critical homeostatic regulator of inflammation that helps terminate TNFα-dependent and TNFα-independent NF-κB activation. A20-null mice develop severe inflammation in many tissues, and die prematurely attributed to hypersensitivity to TNF and Toll-like receptor-4 activation.[53,54] The protective effects of A20 were related to its anti-apoptotic activity, which appears to be stimulus and cell-specific,[55] and to repression of NF-κB activation.[53,56,57] We find that A20 silencing in endothelial-like cells transduced with vFLIP enhances significantly cell growth. Thus, in endothelial cells that express vFLIP, A20 appears to function as an inhibitor of cell growth and an inhibitor of IP-10 chemokine secretion. KSHV vFLIP is a potent inducer of NF-κB target genes and many other pro-inflammatory cytokines. By simultaneously inducing A20 expression, KSHV can temper excessive cell growth and modulate the extent of inflammation surrounding the virus-infected cells, which could be harmful to the virus-infected cells.

Consistent with the results presented here, A20 appears to have the role of a tumor repressor in certain B-lineage tumor cells.[23] A20 is frequently inactivated by somatic mutations or deletions in many types of B-cell lymphomas.[58–60] A20-deficient B-lineage cells generated tumors in immunodeficient mice, but re-expression of A20 reduced their tumorigenicity. In vitro, expression of A20 into a lymphoma-derived cell line deficient of A20 promoted growth arrest and cell death in conjunction with downregulation of NF-κB activation.[58,59]

These results have broadened our understanding of KSHV-vFLIP regulation of endothelial cell growth and chemokine secretion providing evidence for a role of A20 as a modulator of NF-κB activation in the context of KSHV-induced disease pathogenesis.

MATERIALS AND METHODS

Cells

HUVEC were maintained in M199 complete medium, as described.[61] The HUVEC-epithelial A594 hybrid cell line EAHY[62] from American Type Culture Collection (Manassas, VA, USA); the Phoenix cell line (from Dr G Nolan, Stanford University); and the human kidney 293T cell line (gift of Dr H Mitsuya, HIV and AIDS Malignancy Branch, NCI) were cultured in DMEM Glutamax (Invitrogen, Carlsbad, CA, USA) with 10% fetal bovine serum (Atlanta Biologicals, Lawrenceville, GA, USA).

Plasmids

LZRSpBMN-ORFK13-Ires-GFP was described.[21] pTriEX-K13FLAG and pTriEX-K13A57LFLAG were constructed by inserting PCR-amplified K13FLAG and K13A57L-FLAG[21] into the pTriEX1.1/Hyg vector (Merck KGaA, Darmstadt, Germany). For V5-tagged vFLIP, vFLIP was inserted into pLenti6 (Invitrogen). pcDNA3.1-HA-A20, A20 OTU mutant (D100A/C103S) and ABIN-1 were gifts of Dr A Leonardi (University of Naples, Italy).[38] The FLAG-A20 plasmids, pcDNA3.1/Zeo-FLAG-A20, pcDNA3.1/Zeo-A20A103, pcDNA3.1/Zeo-A20ZNF4MT, and pcDNA3.1/ZeoA20ZNF7MT were gifts of Dr R Lin (Jewish General Hospital, Canada).[63] pcDNA3.1-Myc-ABIN-3 was a gift of Dr BK Weaver (Missouri State University).[39] pcDNA3-3 × FLAG-NEMO was provided by Drs JM Peloponese Jr and KT Jeang (National Institutes of Allergy and Infectious Diseases (NIAID), NIH). pNF-κB-Luc was from Clontech (Mountain View, CA, USA). pRL-TK was from Progema (Fitchburg, WI, USA). Restriction enzymes used for plasmid construction were from New England Biolabs (Ipswich, MA, USA).

Antibodies and other reagents

Antibodies were purchased: anti-A20 rabbit polyclonal antibody, anti-Myc tag mouse monoclonal antibody 9E10, anti-HA rabbit polyclonal antibody (Abcam, Cambridge, MA, USA); anti-KSHV LANA/HHV-8 ORF73 rat monoclonal antibody (Advanced Biotechnologies, Columbia, MD, USA); anti-V5 mouse monoclonal antibody (Invitrogen); anti-FLAG mouse monoclonal antibody M2 (Sigma-Aldrich, St. Louis, MI, USA), (Abcam), anti-GFP mouse monoclonal antibody, anti-COX2, anti-HSP90 α/β rabbit polyclonal antibodies and anti-actin goat polyclonal antibody (Santa Cruz Biothechnology, Santa Cruz, CA, USA); anti-IKK1 (IKKα), anti-phosphorylated STAT1 (Tyr701), anti-p100/NF-kB2, anti-RelB, and anti-phopspho-ERK1/2/p44/p42 MAPK (The202/Tyr204) rabbit polyclonal antibodies, anti-ERK1/2p44/p42 MAPK rabbit monoclonal antibody, anti-phosphorylated IκB (Ser32/Ser36), anti-IκB mouse monoclonal antibody, anti-A20 rabbit monoclonal antibody, rabbit IgG anti-ABIN-1/TNFAIP3 (Cell Signaling Technology, Danvers, MA, USA); HRP (horseradish peroxidase)-conjugated anti-rabbit antibody (GE Healthcare, Piscataway, NJ, USA); and HRP-conjugated anti-mouse IgG light chain-specific antibody (Jackson ImmunoResarch Laboratory, West Grove, PA, USA). Recombinant human TNFα was from R&D Systems (Minneapolis, MN, USA).

Retroviral and Lentiviral vFLIP infection; A20, ABIN-1 and IKK1 silencing

Retrovirus for vFLIP and empty control vector expression were prepared as described.[21] Infection rate was evaluated by microscopy and flow cytometry for detection of GFP. Images were taken with Olympus IX51 (Olympus Optical, Melville, NY, USA) equipped with a 120-W mercury lamp (X-cite 120Q; Exfo, Ontario, Canada). Lentivirus for vFLIP and control (pLenti6-LacZ, Invitrogen) were prepared as described.[64] Infection was by spin-inoculation.[65] Selection of vFLIP-expressing cells was achieved by selection with Blasticidin (5 μg/ml). vFLIP expression was evaluated by quantitative RT–PCR. Two

preparations of lentiviral particles for silencing expression of the A20 protein (TRCN0000050958, sequence: 5′-CC GGCGGCTATGACAGCCATCATTTCTCGAGAAATGATGGCTGTCATAGCCGTTTTT G-3′ and TRCN0000050959, sequence: 5′-CCGGGCACCGATACACACTGGAAATCTCGAGATTTCCAGTGTGTATCGGTGCTT TTTG-3′) were purchased from Sigma-Aldrich. Two preparations of lentiviral particles for silencing of ABIN-1 protein (TRCN0000356647, sequence: 5′-CCGGCCACCCAGAAGGCTTTCATTTCTCGAGAAATGAAAGCCTTCTGGGTGGTT TTTG-3′ and TRCN0000378197, sequence: 5′-CCGGTGATGAGCAATGGCAACAAAGCTCGAGCTTTGTTGCCATTG CTCATCATTTTTG-3′) were purchased from Sigma-Aldrich. Control lentiviral particles were produced using non-target shRNA control vector (Sigma-Aldrich). Lentivirus infections were performed by standard techniques.[64] Selection of A20-silenced, ABIN-1-silenced and control cells was achieved by culture with 1 μg/ml Puromycin. ON-TARGET plus SMARTpool siRNAs for human IKK1 and risk-free control siRNA were from Dharmacon, Thermo Scientific (Walthan, MA, USA). Cells were transfected with siRNAs using Oligofectamine reagent (Invitrogen) as described[64] and were tested 72 h after transfection.

RNA extraction, reverse transcription-PCR (RT–PCR) and quantitative PCR

Total RNA was extracted with Trizol (Invitrogen) and purified using RNeasy mini kit (Qiagen, Gaithersburg, MD, USA) after DNase I (Invitrogen) treatment. cDNA from HUVEC was synthesized by Superscript II (Invitrogen) following the manufacturer's protocol; from EAHY cDNA was synthesized by High capacity cDNA Reverse Transcription Kit (Applied Biosystems, Foster City, CA, USA). A20 and vFLIP mRNAs were measured by real-time PCR from 1 μg cDNA with Power Syber green PCR Master Mix (Applied Biosystems). Primer sequences for A20: forward 5′-CG CTGAAAACGAACGGTGAC-3′ and reverse 5′-GGGTATCTGTAGCATTCCTGGG CAG-3′; for vFLIP: forward 5′-CCCTGTTAGGGGAATGTCTGTTTC-3′ and reverse 5′-GTAAGAATGTCTGTGGTGTGCTGC-3′. IP10 and MCP-2 mRNAs were measured by real-time PCR from cDNA amplification of 1 μg RNA with Taqman PCR Universal Master Mix (Applied Biosystems) and Taqman gene expression probes (Applied Biosystems).

Enzyme-linked immunosorbent assay (ELISA)

ELISA for IP-10 and MCP2 were performed with Quantikine Human CXCL10/IP-10 and Human CCL8/MCP2 Duo sets (R&D Systems) according to manufacturer's protocol.

Transfection and luciferase assays

The NF-κB luciferase plasmid (100 ng) and pTK-RL (20 ng) were co-transfected with (500 ng per well) pTriEX-K13FLAG and various amounts of pcDNA-HA-ABIN-1, pcDNA-Myc-ABIN3, or pcDNA-HA-A20 in 12-well plates. Parallel transfections were performed with empty vectors (pTriEX1.1/Hyg and pcDNA3.1(+)mycHisA (Invitrogen)) for normalization. Luciferase assays were performed with the Dual-Luciferase Assay System from Promega. Firefly and Renilla luciferase activities (10 μl from 100 μl total lysate each) were read using the FLUOstar Omega microplate reader (BMG Labtech, Offenburg, Germany). One hundred microliters of luciferase reagent were injected and samples were read sequentially in a luminometer. Luciferase activity was normalized by TK promoter-driven Renilla luciferase activity. Results are expressed as relative luciferase activity.

Immunoprecipitation assays

For immunoprecipitation, pcDNA3-3 × FLAG-NEMO (50 ng/well), pLenti6-vFLIP-V5 (100 ng or 500 ng/well), and various amount of pcDNA3.1-HA-A20 in combinations were mixed for transfection into 293T cells. One day after transfection, cells were harvested and lysed in IP buffer (10 mM of Tris-HCl (pH 7.4), 50 mM of NaCl, 0.1% [v/v] of IGEPAL CA-630 (Sigma-Aldrich), 0.1 mg/ml of bovine serum albumin (BSA) and proteinase inhibitors). Lysates were centrifuged (12 000 r.p.m., 4 °C for 15 min) and rocked (30 min at 4 °C with 10 μl of Protein A agarose, Upstate, Lake Placid, NY, USA). Cleared supernatants were incubated with 0.6 μg of anti-V5 antibody (Invitrogen) and 10 μl of Protein A agarose (Upstate) for 4 h at 4 °C. Beads were washed in IP buffer without BSA, and subjected to western blotting.

Proliferation and viability assays

Cells were seeded at varying densities (2000–30 000 cells/well) in flat-bottom 96-well microtiter plates (Corning Incorporated, Corning, NY, USA) in complete culture medium. Proliferation was measured by evaluating (methyl-^{3}H thymidine uptake 0.6 μCi/well (0.022 MBq/well)); New England Nuclear) during the last 18 h culture of a 2–3 day culture. Viability was measured by trypan blue staining. Each assay was performed in triplicate cultures. The results of proliferation are expressed as mean c.p.m./well.

Immunostaining

Biopsies of cutaneous KS lesions were from patients volunteering on protocols in the HIV and AIDS Malignancy Branch, approved by the Institutional Review Board of the National Cancer Institute; all patients gave written informed consent. AIDS-KS biopsies were fixed (2% paraformaldehyde), incubated in PBS with 15% sucrose overnight, followed by incubation in PBS with 30% sucrose for 1 day in 4 °C, and embedded in optimal cutting temperature compound (Sakura Finetek, Tokyo, Japan), frozen in a dry ice-methyl butanol bath, and kept at − 80 °C. Frozen tissues were sectioned (15 μm thick), placed on glass slides (Histoserv Inc., Germantown, MD, USA) and stored at − 80 °C until use. Slides were fixed with 4% paraformaldehyde for 5 min (room temperature), washed in PBS and soaked in PBS with 0.1% of Triton, 1% of BSA and 5% of fetal bovine serum (PBSTB) for 1 h (room temperature). Sections were incubated with primary antibodies (1:50–1:100 in PBSTB) overnight at 4 °C, washed in PBS three times, followed by incubation with Alexa Fluor 488 and Alexa Fluor 594-conjugated donkey secondary antibodies (Invitrogen, Grand Island, NY, USA, 1:500 dilution; 1 h, room temperature). After washing, samples (mounted with the mounting solution, DAKO, Carpinteria, CA, USA) were visualized through a laser scanning confocal LSM510 microscope fitted with the objective lens Plan Neofluar X25/0.8 (Carl Zeiss MicroImaging, Thornwood, NY, USA). Images were converted into jpeg files by ZEN 2007 Light software (Carl Zeiss MicroImaging).

Statistical analysis

Group differences were evaluated by two-tailed Student's *t*-test. *P* values less than 0.05 were considered significant.

Acknowledgments

We thank G Nolan (Stanford University), BK Weaver (Missouri State University), J-M Peloponese Jr, K-T Jeang (NIAID, NIH), DB Conze, JD Ashwell (NCI, NIH), AV Grishin (University of Southern California), A Leonardi (University of Naples, Italy), R Lin (Jewish General Hospital, Canada) for reagents; the patients who volunteered for this study; Dr MN Polizzotto (NCI, NIH), K Aleman and K Wyvill for patient care; the Confocal Microscopy Core Facility (Laboratory of Experimental Carcinogenesis, CCR, NCI) for providing LSM510 and the DNA Minicore Facility (Laboratory of Experimental Carcinogenesis, CCR, NCI) for DNA sequencing, and K Sakakibara (NCI, NIH) for her help in reporter assay. We also thank Drs D Lowy, O Salvucci, H Ohnuki and all members of

Laboratory of Cellular Oncology Branch for their advice and help on this work. This study was supported by the intramural research program in Center for Cancer Research, National Cancer Institute, National Institutes of Health, Bethesda, MD20892, USA.

References

1. Ambinder, RF.; Cesarman, E. Clinical and pathological aspects of EBV and KSHV infection. In: Arvin, A.; Campadelli-Fiume, G.; Mocarski, E.; Moore, PS.; Roizman, B.; Whitley, R.; Yamanishi, K., editors. Human Herpesviruses: Biology, Therapy, and Immunoprophylaxis. Vol. Chapter 50. Cambridge: Cambridge University Press; 2007.
2. Uldrick TS, Wang V, O'Mahony D, Aleman K, Wyvill KM, Marshall V, et al. An interleukin-6-related systemic inflammatory syndrome in patients co-infected with Kaposi sarcoma-associated herpesvirus and HIV but without Multicentric Castleman disease. Clin Infect Dis. 2010; 51:350–358. [PubMed: 20583924]
3. Schulz, TF.; Chang, Y. KSHV gene expression and regulation. In: Arvin, A.; Campadelli-Fiume, G.; Mocarski, E.; Moore, PS.; Roizman, B.; Whitley, R.; Yamanishi, K., editors. Human Herpesviruses: Biology, Therapy, and Immunoprophylaxis. Vol. Chapter 28. Cambridge: Cambridge University Press; 2007.
4. Grundhoff A, Ganem D. Mechanisms governing expression of the v-FLIP gene of Kaposi's sarcoma-associated herpesvirus. J Virol. 2001; 75:1857–1863. [PubMed: 11160684]
5. Chugh P, Matta H, Schamus S, Zachariah S, Kumar A, Richardson JA, et al. Constitutive NF-kappaB activation, normal Fas-induced apoptosis, and increased incidence of lymphoma in human herpes virus 8 K13 transgenic mice. Proc Natl Acad Sci USA. 2005; 102:12885–12890. [PubMed: 16120683]
6. Ballon G, Chen K, Perez R, Tam W, Cesarman E. Kaposi sarcoma herpesvirus (KSHV) vFLIP oncoprotein induces B cell transdifferentiation and tumorigenesis in mice. J Clin Invest. 2011; 121:1141–1153. [PubMed: 21339646]
7. Chaudhary PM, Jasmin A, Eby MT, Hood L. Modulation of the NF-kappa B pathway by virally encoded death effector domains-containing proteins. Oncogene. 1999; 18:5738–5746. [PubMed: 10523854]
8. Ganem D. KSHV infection and the pathogenesis of Kaposi's sarcoma. Annu Rev Pathol. 2006; 1:273–296. [PubMed: 18039116]
9. Guasparri I, Keller SA, Cesarman E. KSHV vFLIP is essential for the survival of infected lymphoma cells. J Exp Med. 2004; 199:993–1003. [PubMed: 15067035]
10. Liu L, Eby MT, Rathore N, Sinha SK, Kumar A, Chaudhary PM. The human herpes virus 8-encoded viral FLICE inhibitory protein physically associates with and persistently activates the Ikappa B kinase complex. J Biol Chem. 2002; 277:13745–13751. [PubMed: 11830587]
11. Field N, Low W, Daniels M, Howell S, Daviet L, Boshoff C, et al. KSHV vFLIP binds to IKK-gamma to activate IKK. J Cell Sci. 2003; 116(Pt 18):3721–3728. [PubMed: 12890756]
12. Bagneris C, Ageichik AV, Cronin N, Wallace B, Collins M, Boshoff C, et al. Crystal structure of a vFlip-IKKgamma complex: insights into viral activation of the IKK signalosome. Mol Cell. 2008; 30:620–631. [PubMed: 18538660]
13. Hacker H, Karin M. Regulation and function of IKK and IKK-related kinases. Sci STKE. 2006; 2006:re13. [PubMed: 17047224]
14. Harhaj EW, Sun SC. IKKgamma serves as a docking subunit of the IkappaB kinase (IKK) and mediates interaction of IKK with the human T-cell leukemia virus Tax protein. J Biol Chem. 1999; 274:22911–22914. [PubMed: 10438454]
15. Li XH, Fang X, Gaynor RB. Role of IKKgamma/nemo in assembly of the Ikappa B kinase complex. J Biol Chem. 2001; 276:4494–4500. [PubMed: 11080499]
16. Yamaoka S, Courtois G, Bessia C, Whiteside ST, Weil R, Agou F, et al. Complementation cloning of NEMO, a component of the IkappaB kinase complex essential for NF-kappaB activation. Cell. 1998; 93:1231–1240. [PubMed: 9657155]
17. Baeuerle PA, Baltimore D. I kappa B: a specific inhibitor of the NF-kappa B transcription factor. Science. 1988; 242:540–546. [PubMed: 3140380]

18. Grossmann C, Podgrabinska S, Skobe M, Ganem D. Activation of NF-kappaB by the latent vFLIP gene of Kaposi's sarcoma-associated herpesvirus is required for the spindle shape of virus-infected endothelial cells and contributes to their proinflammatory phenotype. J Virol. 2006; 80:7179–7185. [PubMed: 16809323]
19. Matta H, Mazzacurati L, Schamus S, Yang T, Sun Q, Chaudhary PM. Kaposi's sarcoma-associated herpesvirus (KSHV) oncoprotein K13 bypasses TRAFs and directly interacts with the IkappaB kinase complex to selectively activate NF-kappaB without JNK activation. J Biol Chem. 2007; 282:24858–24865. [PubMed: 17597077]
20. Punj V, Matta H, Schamus S, Chaudhary PM. Integrated microarray and multiplex cytokine analyses of Kaposi's sarcoma associated herpesvirus viral FLICE Inhibitory Protein K13 affected genes and cytokines in human blood vascular endothelial cells. BMC Med Genomics. 2009; 2:50. [PubMed: 19660139]
21. Sakakibara S, Pise-Masison CA, Brady JN, Tosato G. Gene regulation and functional alterations induced by Kaposi's sarcoma-associated herpesvirus-encoded ORFK13/vFLIP in endothelial cells. J Virol. 2009; 83:2140–2153. [PubMed: 19091861]
22. Thurau M, Marquardt G, Gonin-Laurent N, Weinlander K, Naschberger E, Jochmann R, et al. Viral inhibitor of apoptosis vFLIP/K13 protects endothelial cells against superoxide-induced cell death. J Virol. 2009; 83:598–611. [PubMed: 18987137]
23. Matta H, Gopalakrishnan R, Punj V, Yi H, Suo Y, Chaudhary PM. A20 is induced by Kaposi sarcoma-associated herpesvirus-encoded viral FLICE inhibitory protein (vFLIP) K13 and blocks K13-induced nuclear factor-kappaB in a negative feedback manner. J Biol Chem. 2011; 286:21555–21564. [PubMed: 21531730]
24. Opipari AW Jr, Boguski MS, Dixit VM. The A20 cDNA induced by tumor necrosis factor alpha encodes a novel type of zinc finger protein. J Biol Chem. 1990; 265:14705–14708. [PubMed: 2118515]
25. Opipari AW Jr, Hu HM, Yabkowitz R, Dixit VM. The A20 zinc finger protein protects cells from tumor necrosis factor cytotoxicity. J Biol Chem. 1992; 267:12424–12427. [PubMed: 1618749]
26. Cooper JT, Stroka DM, Brostjan C, Palmetshofer A, Bach FH, Ferran C. A20 blocks endothelial cell activation through a NF-kappaB-dependent mechanism. J Biol Chem. 1996; 271:18068–18073. [PubMed: 8663499]
27. Krikos A, Laherty CD, Dixit VM. Transcriptional activation of the tumor necrosis factor alpha-inducible zinc finger protein, A20, is mediated by kappa B elements. J Biol Chem. 1992; 267:17971–17976. [PubMed: 1381359]
28. Verstrepen L, Verhelst K, van Loo G, Carpentier I, Ley SC, Beyaert R. Expression, biological activities and mechanisms of action of A20 (TNFAIP3). Biochem Pharmacol. 2010; 80:2009–2020. [PubMed: 20599425]
29. Wertz IE, O'Rourke KM, Zhou H, Eby M, Aravind L, Seshagiri S, et al. De-ubiquitination and ubiquitin ligase domains of A20 downregulate NF-kappaB signalling. Nature. 2004; 430:694–699. [PubMed: 15258597]
30. Harhaj EW, Dixit VM. Deubiquitinases in the regulation of NF-kappaB signaling. Cell Res. 2010; 21:22–39. [PubMed: 21119682]
31. O'Reilly SM, Moynagh PN. Regulation of Toll-like receptor 4 signalling by A20 zinc finger protein. Biochem Biophys Res Commun. 2003; 303:586–593. [PubMed: 12659860]
32. De Valck D, Jin DY, Heyninck K, Van de Craen M, Contreras R, Fiers W, et al. The zinc finger protein A20 interacts with a novel anti-apoptotic protein which is cleaved by specific caspases. Oncogene. 1999; 18:4182–4190. [PubMed: 10435631]
33. Heyninck K, De Valck D, Vanden Berghe W, Van Criekinge W, Contreras R, Fiers W, et al. The zinc finger protein A20 inhibits TNF-induced NF-kappaB-dependent gene expression by interfering with an RIP- or TRAF2-mediated transactivation signal and directly binds to a novel NF-kappaB-inhibiting protein ABIN. J Cell Biol. 1999; 145:1471–1482. [PubMed: 10385526]
34. Shembade N, Parvatiyar K, Harhaj NS, Harhaj EW. The ubiquitin-editing enzyme A20 requires RNF11 to downregulate NF-kappaB signalling. EMBO J. 2009; 28:513–522. [PubMed: 19131965]

35. Song HY, Rothe M, Goeddel DV. The tumor necrosis factor-inducible zinc finger protein A20 interacts with TRAF1/TRAF2 and inhibits NF-kappaB activation. Proc Natl Acad Sci USA. 1996; 93:6721–6725. [PubMed: 8692885]
36. Wullaert A, Verstrepen L, Van Huffel S, Adib-Conquy M, Cornelis S, Kreike M, et al. LIND/ABIN-3 is a novel lipopolysaccharide-inducible inhibitor of NF-kappaB activation. J Biol Chem. 2007; 282:81–90. [PubMed: 17088249]
37. Wagner S, Carpentier I, Rogov V, Kreike M, Ikeda F, Lohr F, et al. Ubiquitin binding mediates the NF-kappaB inhibitory potential of ABIN proteins. Oncogene. 2008; 27:3739–3745. [PubMed: 18212736]
38. Mauro C, Pacifico F, Lavorgna A, Mellone S, Iannetti A, Acquaviva R, et al. ABIN-1 binds to NEMO/IKKgamma and co-operates with A20 in inhibiting NF-kappaB. J Biol Chem. 2006; 281:18482–18488. [PubMed: 16684768]
39. Weaver BK, Bohn E, Judd BA, Gil MP, Schreiber RD. ABIN-3: a molecular basis for species divergence in interleukin-10-induced anti-inflammatory actions. Mol Cell Biol. 2007; 27:4603–4616. [PubMed: 17485448]
40. Shembade N, Ma A, Harhaj EW. Inhibition of NF-kappaB signaling by A20 through disruption of ubiquitin enzyme complexes. Science. 2010; 327:1135–1139. [PubMed: 20185725]
41. Ohmori Y, Hamilton TA. Cooperative interaction between interferon (IFN) stimulus response element and kappa B sequence motifs controls IFN gamma- and lipopolysaccharide-stimulated transcription from the murine IP-10 promoter. J Biol Chem. 1993; 268:6677–6688. [PubMed: 8454640]
42. Zhang SQ, Kovalenko A, Cantarella G, Wallach D. Recruitment of the IKK signalosome to the p55 TNF receptor: RIP and A20 bind to NEMO (IKKgamma) upon receptor stimulation. Immunity. 2000; 12:301–311. [PubMed: 10755617]
43. Guasparri I, Wu H, Cesarman E. The KSHV oncoprotein vFLIP contains a TRAF-interacting motif and requires TRAF2 and TRAF3 for signalling. EMBO Rep. 2006; 7:114–119. [PubMed: 16311516]
44. Stilo R, Varricchio E, Liguoro D, Leonardi A, Vito P. A20 is a negative regulator of BCL10- and CARMA3-mediated activation of NF-kappaB. J Cell Sci. 2008; 121(Pt 8):1165–1171. [PubMed: 18349075]
45. Ea CK, Deng L, Xia ZP, Pineda G, Chen ZJ. Activation of IKK by TNFalpha requires site-specific ubiquitination of RIP1 and polyubiquitin binding by NEMO. Mol Cell. 2006; 22:245–257. [PubMed: 16603398]
46. Rahighi S, Ikeda F, Kawasaki M, Akutsu M, Suzuki N, Kato R, et al. Specific recognition of linear ubiquitin chains by NEMO is important for NF-kappaB activation. Cell. 2009; 136:1098–1109. [PubMed: 19303852]
47. Yoshikawa A, Sato Y, Yamashita M, Mimura H, Yamagata A, Fukai S. Crystal structure of the NEMO ubiquitin-binding domain in complex with Lys 63-linked di-ubiquitin. FEBS Lett. 2009; 583:3317–3322. [PubMed: 19766637]
48. Hadian K, Griesbach RA, Dornauer S, Wanger TM, Nagel D, Metlitzky M, et al. NF-{kappa}B Essential Modulator (NEMO) interaction with linear and Lys-63 ubiquitin chains contributes to NF-{kappa}B activation. J Biol Chem. 2011; 286:26107–26117. [PubMed: 21622571]
49. Matta H, Sun Q, Moses G, Chaudhary PM. Molecular genetic analysis of human herpes virus 8-encoded viral FLICE inhibitory protein-induced NF-kappaB activation. J Biol Chem. 2003; 278:52406–52411. [PubMed: 14561765]
50. Shembade N, Pujari R, Harhaj NS, Abbott DW, Harhaj EW. The kinase IKKalpha inhibits activation of the transcription factor NF-kappaB by phosphorylating the regulatory molecule TAX1BP1. Nat Immunol. 2011; 12:834–843. [PubMed: 21765415]
51. Li Q, Lu Q, Bottero V, Estepa G, Morrison L, Mercurio F, et al. Enhanced NF-kappaB activation and cellular function in macrophages lacking IkappaB kinase 1 (IKK1). Proc Natl Acad Sci USA. 2005; 102:12425–12430. [PubMed: 16116086]
52. Liu B, Yang Y, Chernishof V, Loo RR, Jang H, Tahk S, et al. Proinflammatory stimuli induce IKKalpha-mediated phosphorylation of PIAS1 to restrict inflammation and immunity. Cell. 2007; 129:903–914. [PubMed: 17540171]

53. Lee EG, Boone DL, Chai S, Libby SL, Chien M, Lodolce JP, et al. Failure to regulate TNF-induced NF-kappaB and cell death responses in A20-deficient mice. Science. 2000; 289:2350–2354. [PubMed: 11009421]
54. Boone DL, Turer EE, Lee EG, Ahmad RC, Wheeler MT, Tsui C, et al. The ubiquitin-modifying enzyme A20 is required for termination of Toll-like receptor responses. Nat Immunol. 2004; 5:1052–1060. [PubMed: 15334086]
55. Daniel S, Arvelo MB, Patel VI, Longo CR, Shrikhande G, Shukri T, et al. A20 protects endothelial cells from TNF-, Fas-, and NK-mediated cell death by inhibiting caspase 8 activation. Blood. 2004; 104:2376–2384. [PubMed: 15251990]
56. Beyaert R, Heyninck K, Van Huffel S. A20 and A20-binding proteins as cellular inhibitors of nuclear factor-kappa B-dependent gene expression and apoptosis. Biochem Pharmacol. 2000; 60:1143–1151. [PubMed: 11007952]
57. Natoli G, Costanzo A, Guido F, Moretti F, Bernardo A, Burgio VL, et al. Nuclear factor kB-independent cytoprotective pathways originating at tumor necrosis factor receptor-associated factor 2. J Biol Chem. 1998; 273:31262–31272. [PubMed: 9813034]
58. Kato M, Sanada M, Kato I, Sato Y, Takita J, Takeuchi K, et al. Frequent inactivation of A20 in B-cell lymphomas. Nature. 2009; 459:712–716. [PubMed: 19412163]
59. Compagno M, Lim WK, Grunn A, Nandula SV, Brahmachary M, Shen Q, et al. Mutations of multiple genes cause deregulation of NF-kappaB in diffuse large B-cell lymphoma. Nature. 2009; 459:717–721. [PubMed: 19412164]
60. Giulino L, Mathew S, Ballon G, Chadburn A, Barouk S, Antonicelli G, et al. A20 (TNFAIP3) genetic alterations in EBV-associated AIDS-related lymphoma. Blood. 2011; 117:4852–4854. [PubMed: 21406721]
61. Narazaki M, Tosato G. Ligand-induced internalization selects use of common receptor neuropilin-1 by VEGF165 and semaphorin3A. Blood. 2006; 107:3892–3901. [PubMed: 16424390]
62. Edgell CJ, McDonald CC, Graham JB. Permanent cell line expressing human factor VIII-related antigen established by hybridization. Proc Natl Acad Sci USA. 1983; 80:3734–3737. [PubMed: 6407019]
63. Lin R, Yang L, Nakhaei P, Sun Q, Sharif-Askari E, Julkunen I, et al. Negative regulation of the retinoic acid-inducible gene I-induced antiviral state by the ubiquitin-editing protein A20. J Biol Chem. 2006; 281:2095–2103. [PubMed: 16306043]
64. Salvucci O, Maric D, Economopoulou M, Sakakibara S, Merlin S, Follenzi A, et al. EphrinB reverse signaling contributes to endothelial and mural cell assembly into vascular structures. Blood. 2009; 114:1707–1716. [PubMed: 19411631]
65. Sakakibara S, Sakakibara K, Tosato G. NF-kappaB activation stimulates transcription and replication of retrovirus XMRV in human B-lineage and prostate carcinoma cells. J Virol. 2011; 85:3179–3186. [PubMed: 21270144]

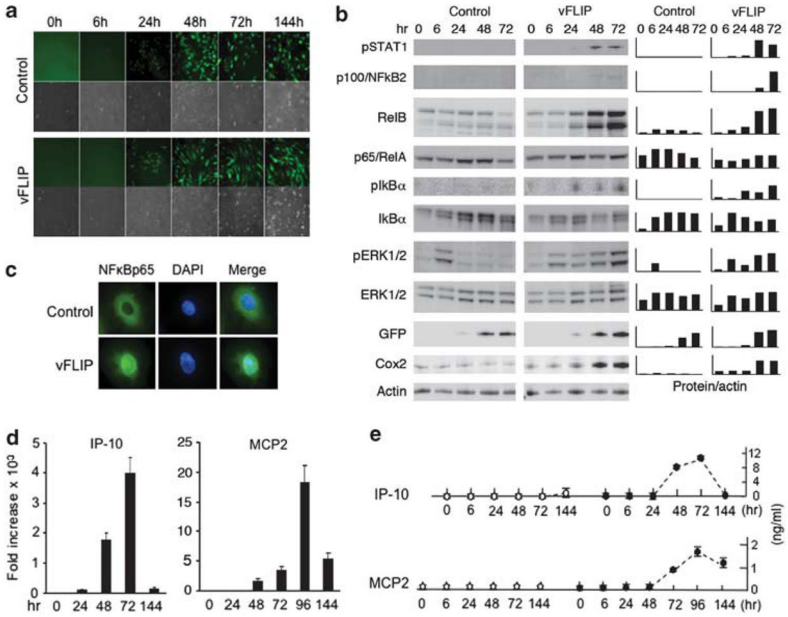

Figure 1.

Early events following vFLIP transduction of primary human endothelial cells. (**a**) HUVEC were transduced with either the vFLIP-expressing retroviral vector *ORFK13-IRES-Gfp* or the empty vector *IRES-Gfp*. The representative fluorescence and phase-contrast microscopy images show evidence of retroviral infection, reflected by the green fluorescence and change in cell morphology (original magnification × 100). (**b**) Kinetic analysis of vFLIP-induced expression of phospho-STAT1 (Tyr701), p100/NF-κB2, RelB, p65/RelA, phospho-IkBα, IkBα, phospho-ERK1/2, ERK1/2, GFP, Cox2 and actin detected by western blotting (WB) of HUVEC lysates. (**c**) Nuclear localization of NFκBp65 protein in vFLIP-expressing but not control HUVEC detected by immunofluorescence staining. HUVEC were tested 3 days after vFLIP transduction. Original magnification 100 ×. (**d**) Kinetics of IP-10 and MCP2 mRNA expression in vFLIP-transduced or control-transduced HUVEC detected by quantitative PCR analysis. The results reflect the means of triplicate determinations, representative of three experiments performed. (**e**) Kinetics of IP-10 and MCP2 protein secretion in the culture supernatant of HUVEC transduced with vector only (open circles) or vFLIP (black circles) detected by specific ELISAs. The results reflect the means (±s.d.) of triplicate cultures.

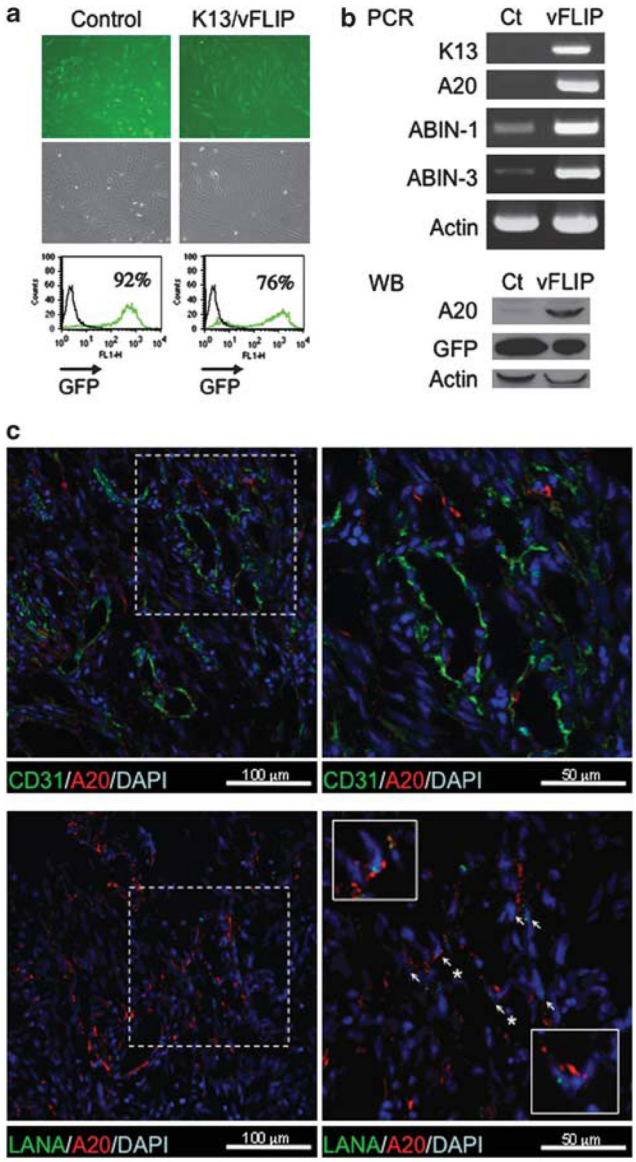

Figure 2.

vFLIP transduction in primary endothelial cells induces A20, ABIN-1 and ABIN-3 mRNAs. (**a**) HUVEC infected with control (*IRES-Gfp*) or vFLIP (*ORFK13-IRES-Gfp*) retrovirus detected by GFP fluorescent microscopy (top) and flow cytometry (bottom) were examined in parallel (**b**) for expression of A20, ABIN-3 and actin mRNAs by RT–PCR (top), and for A20, GFP and actin proteins by western blotting (bottom). (**c**) A20 expression in KS tissues. Upper panels: KS tissue was stained with anti-A20 rabbit polyclonal antibody and anti-CD31 mouse monoclonal antibody (the right panel is a magnification of the boxed area on the left); nuclei are visualized by DAPI. Lower panels: KS tissue was stained with anti-A20 rabbit polyclonal antibody and anti-LANA rat monoclonal antibody; nuclei are visualized by DAPI (the right panel is a magnification of the boxed area on the left; the two boxed squares within the right panel are further magnifications) Magnified areas are outlined with white dotted or continuous lines. Arrows point to representative cells expressing both LANA and A20. Original magnification 60 ×.

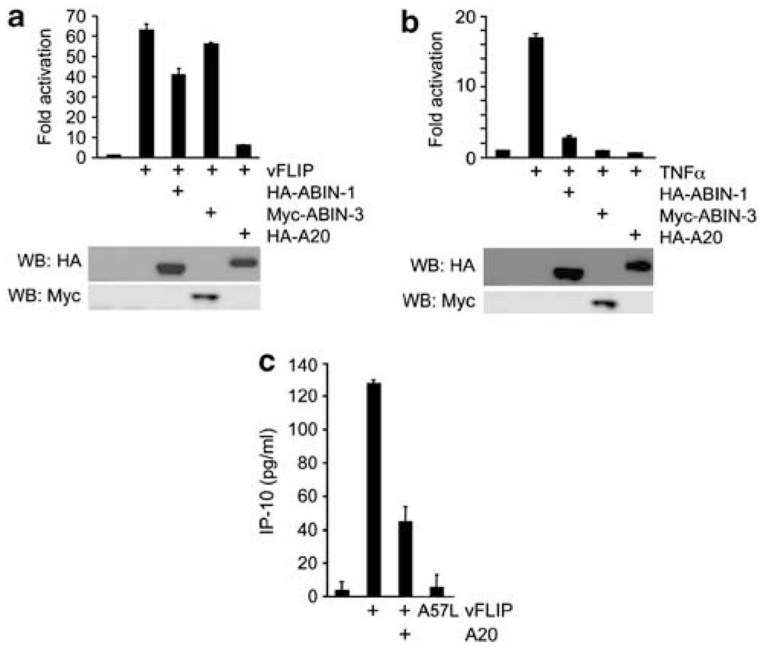

Figure 3.

A20 inhibits vFLIP-induced NF-κB activation. (**a**) The NF-κB-Luc reporter plasmid was co-transfected in 293T cells with expression plasmids for vFLIP (500 ng/well) ABIN-1, ABIN-3 or A20 (each, 500 ng/well). After 16 h incubation, luciferase activity was measured by the dual-luciferase assay system; the results are expressed as fold activation compared with luciferase activity in cell transfected with the luciferase reporter and empty vectors. Expression of HA-ABIN-1, HA-A20 and Myc-ABIN-3 was detected by immunoblotting the cell lysates with anti-HA or anti-Myc specific antibodies (shown below the bar graph). The assays were performed in triplicate; the results are representative of three experiments performed. (**b**) The NF-κB-Luc reporter plasmid was co-transfected in 293T cells with expression plasmids for ABIN-1, ABIN-3 or A20 (each, 500 ng/well). TNFα (10ng/ml) was added to the 293T cell culture immediately after transfection. The immunoblot below the bar graph documents expression of ABIN-1, ABIN-3 and A-20 by using antibodies to the HA or Myc tags. The assays were performed in triplicate; the results are representative of three independent experiments performed. Protein expression of the transduced plasmids was confirmed by western blotting shown below the bar graphs. (**c**) Levels of IP-10 detected by ELISA in the conditioned media of 293T cells transduced 24 h earlier with vFLIP, the vFLIP A57L mutant (which is defective at binding to NEMO), or vFLIP plus A20. IP-10 measurements were performed in duplicate and representative results from three independent experiments are shown.

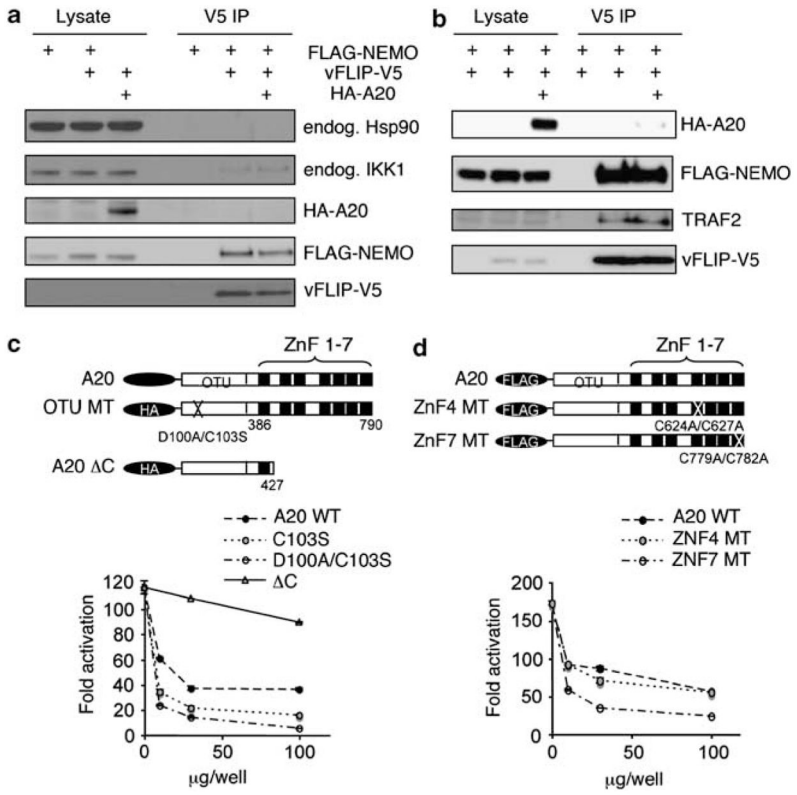

Figure 4.

A20 does not alter vFLIP-NEMO and vFLIP-TRAF2 interactions; the OTU domain and the zinc finger domain 4 do not contribute to A20 inhibition of vFLIP-induced NF-κB activation. (**a** and **b**) Immunoprecipitation assays. The 293T cells were transfected with FLAG-tagged NEMO (10 ng/well) alone, with FLAG-NEMO plus V5-tagged vFLIP (vFLIP-V5), or with FLAG-NEMO plus K13-V5 plus HA-tagged A20 (HA-A20). Cell lysates were analyzed before (Lysate) or after immunoprecipitation with anti-V5 antibody (V5 IP) followed by protein A agarose for 4 h at 4 °C. Antibody-bound beads were washed in lysis buffer five times and precipitated proteins were analyzed by western blotting with the indicated specific antibodies. Representative results from three experiments each. (**c**) Top: schematic representation of A20: full-length HA-tagged WT A20 plasmid containing the WT OTU motif and the WT zinc finger motifs (ZnF) 1–7; OTU mutants: HA-tagged A20 OTU mutants C103S (cysteine 103 replaced by serine) and D100A/C103S (aspartic acid 100 replaced by alanine and cysteine 103 replaced by serine; the C-terminal deletion (aa 428–790) mutant; and ΔC: HA-tagged C-terminal deletion 428–790 mutant. Bottom: the full-length WT A20 plasmid (A20 WT), A20 OTU mutants C103S and D100A/C103S, and the C-terminal deletion 428–790 mutant (ΔC) (100, 30, 10 ng/well each) were tested in NF-κB reporter assays after transfection of the vFLIP plasmid (500 ng/well) in 293T cells. (**d**) Top: schematic representation of A20: FLAG-tagged WT A20 plasmid (A20); ZNF4MT: FLAG-tagged A20 zinc finger 4 mutants C624A/C627A (cysteine 624 replaced by alanine and cysteine 627 replaced by alanine); and ZNF7 MT: FLAG-tagged A20 zinc finger 7 mutant C779A/C782A (cysteine 779 replaced by alanine and cysteine 782 replaced by alanine). Bottom: the WT A20 plasmid (A20 WT), the A20 zinc finger mutants ZNF4 and ZNF7 (100, 30, 10 ng/well each) were tested in NF-κB reporter assays after 293T cell transfection with the vFLIP plasmid (500 ng/well). For results shown in **c** and **d**, the reporter assays were performed in duplicate and representative results from three independent experiments are shown.

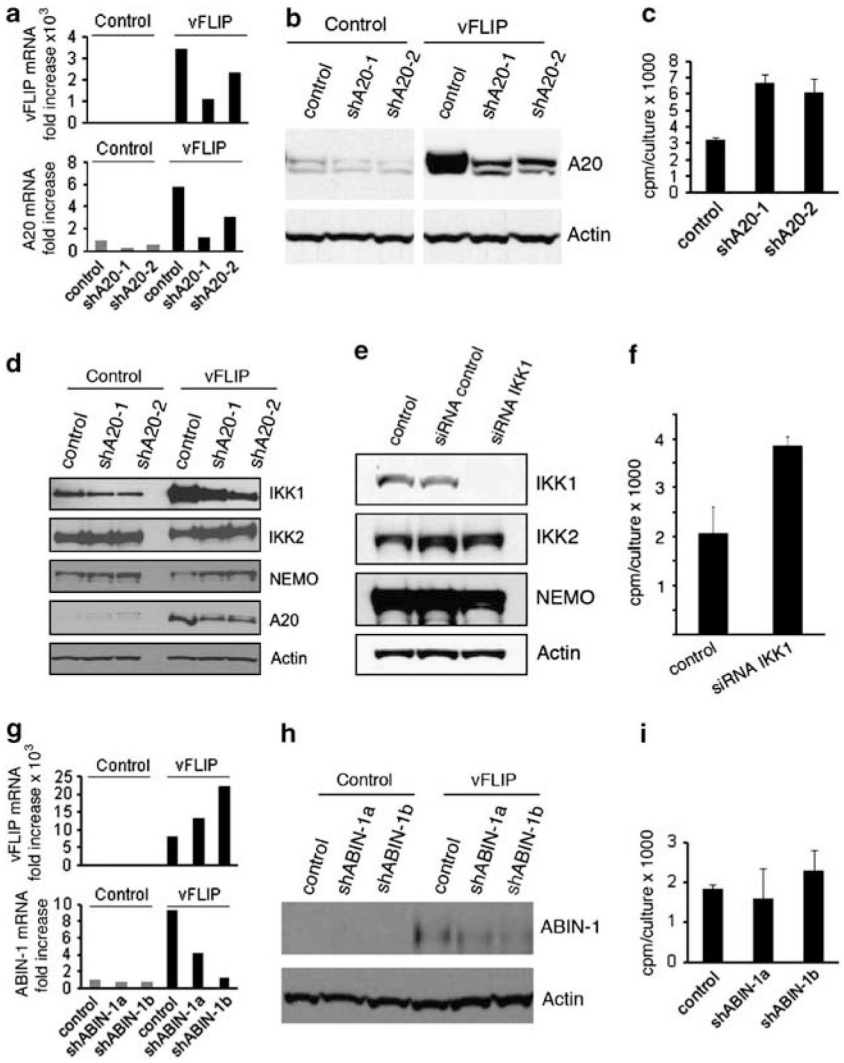

Figure 5.

A20 and IKK1 silencing, but not ABIN-1 silencing, enhances the proliferation of vFLIP-expressing endothelial cells. (**a**) Relative expression of vFLIP (top) and A20 (bottom) mRNAs in EAHY cells transduced with control vector (control) or vFLIP-lentivirus (vFLIP) and further transduced with A20-silencing lentiviral vectors (shA20-1 and shA20-2) or a control lentivirus; selection was performed with Blasticidin (vFLIP and control) and Puromycin (A20 silencing and control). The results are from quantitative PCR. (**b**) A20 protein detected by immunoblotting in EAHY cells transduced with control or vFLIP lentivirus, and subsequently transduced with A20-silencing lentiviral vectors or a control vector. Note that the two panels reflect different exposure times to account for increased levels of A20 in vFLIP-expressing cells. The membranes were re-probed for actin as a loading control. (**c**) Proliferation in vFLIP-expressing EAHY cells in which A20 was silenced (shA20-1 or shA20-2) in comparison with control silenced cells (control). All cells were incubated (12.5×10^5 cells/ml; 96-well plates) for 18 h in the presence of ^{3}H-thymidine. The results reflect the mean cpm/culture (±s.d.) from three experiments, each performed in triplicate. (**d**) IKK1, IKK2 and NEMO proteins detected by immunoblotting in EAHY cells transduced with vFLIP lentivirus or control, and further transduced with a control or A20 silencing lentivirus (shA20-1 or shA20-2). The cells were cultured for ≥4

weeks after selection with Blasticidin and Puromycin. (**e**) Reduction of IKK1 protein levels in vFLIP-expressing EAHY cells resulting from SMARTpool IKK1 siRNA transfection. Immunoblotting results. Control: lipofectamine only; control siRNA: Risk-free siRNA control. (**f**) Proliferation in IKK1-silenced EAHY cells expressing vFLIP. Control: Risk-free siRNA control. The culture conditions are those described for panel c. The results are expressed as mean cpm/culture (±s.d.) from three independent experiments, each performed in triplicate. (**g**) Relative expression of vFLIP (top) and ABIN-1 (bottom) mRNAs in EAHY cells transduced with control vector (control) or vFLIP-lentivirus (vFLIP) and further transduced with ABIN-1 silencing lentiviral vectors (shABIN-1a and shABIN-1b) or control lentivirus. The results are from quantitative PCR after Blasticidin (vFLIP) and Puromycin (ABIN-1) selection. (**h**) ABIN-1 protein detected by immunoblotting of EAHY cells transduced with control or vFLIP lentivirus and further transduced with ABIN-1 silencing lentiviral vectors or control lentivirus. Actin levels serve as a loading control. (**i**) Proliferation of EAHY cells transduced with vFLIP lentivirus and further transduced with the ABIN-1 silencing vectors shABIN-1a, shABIN-1b or with control lentivirus. The culture conditions are those described for panel c. The results reflect the mean c.p.m./culture (±s.d.) from three experiments.